Modeling Uncertainty of Runoff and Sediment Yield Using a Distributed Hydrologic Model

Mohamed M. Hantush, Latif Kalin

Abstract

The event- and physically-based runoff and erosion model KINEROS2 is applied to assess the impact of uncertainty in model parameters on simulated hydrographs and sediment discharge in a small experimental watershed. The net capillary drive parameter, which affects soil infiltration, is shown to be approximately lognormally distributed, and related statistics of this parameter for all soil texture class are computed and tabulated. The model output response to uncertainty in soil hydraulic and channel roughness parameters is evaluated by performing Monte Carlo (MC) simulations based on the parameters' statistics obtained from the literature. The results show the extent to which uncertainty in the saturated hydraulic conductivity, net capillary drive, and initial relative saturation influences the simulated cumulative distributions of peak sediment discharge and sediment yield. The distribution of the simulated time to peak sediment discharge is dominated by uncertainty in the channel and plane Manning's roughness coefficients. Comparison of the simulated median and uncertainty (± 25% and 45% quartiles) with observed values of runoff and sediment discharge, for two, large and small rainfall events, indicate that the model performs properly and can be calibrated based on the range of soil parameters reported in the literature.

Keywords: Sediment, Hydrologic model, KINEROS2, Monte Carlo simulations, uncertainty, net capillary drive

Hantush is a research hydrologist, U.S. EPA, National Risk Management Research Laboratory, OH 45268. E-mail: hantush.mohamed@epa.gov. Kalin is an ORISE postdoctoral researcher, U.S. EPA, National Risk Management Research Laboratory, OH 45268. E-mail: kalin.latif@epa.gov

Introduction

Sediments are cited as the third leading cause of stress for lakes, reservoirs, and ponds, behind nutrients and metals (USEPA 2000). Agriculture land use activities are the leading source for sediment stress. Sediment runoff carries with it adsorbed toxic chemicals and nutrients that have the potential to cause major environmental problems to aquatic ecological systems and water quality impairment in streams and lakes (e.g., eutrophication and hypoxia). Distributed hydrologic runoff/sediment models are increasingly relied upon by scientists and resource managers as cost-effective tools for linking hillslope soil erosion and erodable surfaces to receiving waterbodies, thereby, allowing for direct assessment of the impact of land use practices on water quality in streams and lakes.

The Kinematic Runoff and Erosion model KINEROS2, which is based on first principals (i.e., physics based), is suitable for evaluating the effect of events on runoff and erosion in small watersheds (*Smith et al*. 1995). In spite of its limitations, successful applications of this model to gaged watersheds has been reported in the literature (*Osborn and Simanton* 1990, *Goodrich et al*. 1994, *Smith et al*. 1999, *Ziegler et al*. 2001, *Kalin et al*. 2003, and *Kalin and Hantush* 2003). This paper presents an application to the event-based model KINEROS2 to simulate runoff and sediment discharge in a USDA experimental watershed. The objectives are: i) to identify model parameters that contribute mostly to model output uncertainty by performing Monte Carlo simulations; and ii) estimating uncertainties in model predictions.

Background Theory

KINEROS2 is a distributed, event-oriented, physically based model describing the processes of surface runoff and erosion from small agricultural and urban

watersheds (*Woolhiser et al*. 1990). The watershed is represented by cascade of planes and channels, in which flow and sediments are routed from one plane to the other and, ultimately, to the channels. The cascades allow rainfall, infiltration, runoff, and erosion parameters to vary spatially. This model may be used to determine the effects of various artificial features such as urban developments, small detention reservoirs, or lined channels on flood hydrographs and sediment yield.

When rainfall rate approaches the infiltration capacity, Hortonian overland flow begins. KINEROS2 assumes one-dimensional flow in each plane and solves the kinematic wave approximation of the overland and channel flow equations using finite differences. The flow rate is related to the channel flow cross-sectional area or overland flow depth through Chezy and Manning flow resistance relationships. In these relationships the channel or bed slope approximates the friction slope.

Sediment transport equation is described by the following mass balance equation:

$$\frac{\partial}{\partial t}(AC) + \frac{\partial}{\partial x}(QC) - e(x,t) = q_s(x,t) \qquad (1)$$

in which C is the volumetric sediment concentration [L^3/L^3]; A is the channel cross section area [L^2]; for overland flow it is equal to the flow depth h for a unit flow width [L]; Q is the is the channel discharge [L^3/T]; for overland flow it is equal to the discharge per unit width [L^2/T]; e is sediment erosion rate [L^2/T] given below; and q_s is the rate of lateral sediment inflow for channels [$L^3/T/L$]. In KINEROS2 Sediment erosion/deposition rate e is composed of rainfall splash erosion rate g_s and hydraulic erosion rate g_h:

$$e = g_s + g_h \qquad (2)$$

Rainfall splash erosion is given by (Woolhiser et al., 1990)

$$\begin{aligned} g_s &= c_f\, e^{-c_h h}\, r\, q; & q > 0 \\ &= 0; & q < 0 \end{aligned} \qquad (3)$$

in which c_f is a positive constant [T]; h is flow depth [L]; c_h is damping coefficient for splash erosion [L^{-1}]; r is rainfall rate [L/T]; q is excess rainfall (rainfall rate minus interception minus infiltration) [L/T]. The exponential term represents the reduction in splash erosion caused by increasing depth of water (*Smith et al*. 1995). In channel flow, this term is usually equal to zero: the accumulating water depth absorbs nearly all the imparted energy by the raindrops. The hydraulic erosion represents the rate of exchange of sediment between the flowing water and the soil over which it flows. Such interplay between shear force of water on the loose soil or channel bed and the tendency of the soil particles to settle under the force of gravity may be described by this first-order rate expression:

$$g_h = c_g(C^* - C)\,A \qquad (4)$$

in which C^* is the volumetric concentration at equilibrium transport capacity [L^3/L^3]; c_g is a transfer rate coefficient [T^{-1}]. For sheet flow A = h. This relationship assumes that if C exceeds equilibrium saturation, C^*, deposition occurs. c_g is usually very high for fine, noncohesive material, and very low for cohesive material. Several expressions for C^* are available from literature (see, e.g., *Woolhiser et al*. 1990). In our analysis, we used *Engelund and Hansen* (1967) formula.

Net Capillary Drive Parameter

At the beginning of a storm and prior to ponding, the infiltration rate is rain limited and equal to the rate of precipitation. At the onset of ponding, the infiltration rate is equal to the infiltration capacity, provided that it is greater than the saturated hydraulic conductivity of the soil, and is given by (*Parlange et al.* 1982):

$$f(t) = K_s\left[1 + \frac{\alpha}{e^{\alpha F(t)/[(G+h)(\theta_s - \theta_i)]} - 1}\right] \qquad (5)$$

in which f(t) is the infiltration capacity [L/T]; F(t) is the cumulative depth of the water infiltrated into the soil [L]; θ_s is the soil porosity [L^3/L^3]; θ_i is the initial soil moisture content prior to the storm; α is a parameter generally between 0 and 1; and K_s is the soil saturated hydraulic conductivity [L/T]. $\alpha = 0$ corresponds to the familiar Green Ampt infiltration method. For most soils, $\alpha = 0.85$ has been recommended (*Parlange et al*. 1982). G is the net capillary drive parameter:

$$G = \int_0^{\psi_i} [K(\psi)/K_s]\, d\psi \qquad (6)$$

ψ here is defined as the negative of the capillary pressure [L]. If we substitute the Brooks and Corey soil characteristic relation for unsaturated conductivity:

$$K(\psi) = K_s \left(\psi_b / \psi\right)^{2+3\lambda} \quad (7)$$

and integrate from 0 to ψ_b, with $K(\psi) = K_s$ and from ψ_b to ψ_i, with $K(\psi)$ given by (7)we obtain

$$G = \psi_b \left\{ 1 + \frac{1 - (\psi_b / \psi_i)^{1+3\lambda}}{1 + 3\lambda} \right\} \quad (8)$$

in which ψ_b is the bubbling pressure [L]; ψ_i is the negative of the soil initial capillary head [L]; and λ is the pore-size distribution index. The specific case of $\psi_i = \infty$ produces the commonly used expression for the net capillary drive function $G = \psi_b [(2+3\lambda)/(1+3\lambda)]$. This expression is used in KINEROS2, which may be valid after prolonged rainfall hiatus. For relatively wet soil conditions or short hiatus periods, the capillary pressure may attain a finite, but not a large absolute value. The effect of this on runoff and sediment yield hitherto is unknown. Figure 1 shows variation of the scaled net capillary drive G/ψ_b with scaled initial capillary pressure head ψ_b/ψ_i for soil textures loamy sand ($\lambda = 0.553$), silt loam ($\lambda = 0.234$), and silt clay ($\lambda = 0.15$). Values for λ shown in the figure are the arithmetic means (*Rawls et al*. 1982). Note that for sufficiently wet silty clay, arithmetic mean $\psi_b = 76.54$ cm (*Rawls et al*. 1982), G would be quite different, say, at $\psi_b/\psi_i = 0.7$ than at 0. For example, at $\psi_i = \infty$, $G = 1.69 \times 76.54 \approx 129$ cm; at $\psi_i = 109$ cm, $G = 1.28 \times 76.54 \approx 98$ cm. The use of G value based on $\psi_i = \infty$ may lead to over predicting infiltration and under predicting runoff, consequently, sediment yield.

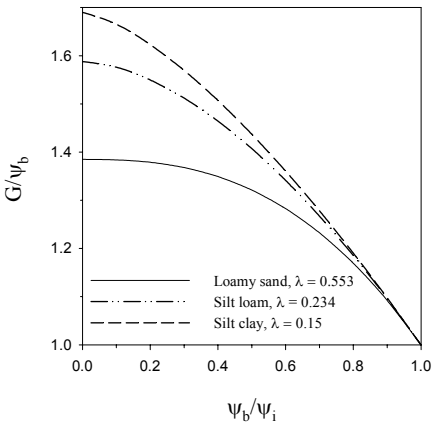

Figure 1. Scaled net capillary drive versus scaled initial capillary pressure for three different soil textures.

To achieve the above two objectives, we begin by developing the probability density function for the G parameter, using the commonly used expression $G = \psi_b[(2+3\lambda)/(1+3\lambda)]$, while bearing in mind that in general G may also depend on the initial capillary pressure ψ_i through Equation (8) (refer to Figure 1). Taking the natural logarithm of both sides of the above expression (G at $\psi_i = \infty$) leads to

$$\ln G = \ln \psi_b + \ln\left(\frac{2+3\lambda}{1+3\lambda}\right) \quad (9)$$

Rawls et al. (1982) indicated that ψ_b and λ are log-normally distributed; they provided the arithmetic and geometric mean values with the corresponding standard deviations for both parameters, for different texture class. Over the reported range of values for λ, we have this approximation: $\ln G \sim N(\mu_{\ln G}, \sigma^2_{\ln \psi_b})$,

$$\mu_{\ln G} \approx \mu_{\ln \psi_b} + \ln\left[(2+3\bar{\lambda})/(1+3\bar{\lambda})\right] \quad (10)$$

That is; G is **lognormally** distributed, with the mean of lnG (i.e., geometric mean) given by (10) and variance of $\ln G \approx \sigma^2_{\ln \psi_b}$, which is the variance of $\ln \psi_b$. $\bar{\lambda}$ is the geometric mean of λ. *Rawls et al*. (1982) provide values of $\sigma^2_{\ln \psi_b}$ and $\bar{\lambda}$ for different soil textures. Table 1 provides the arithmetic mean and standard deviations of G for different soil textures obtained from the lognormal approximation and by performing 10000 Monte Carlo simulations, using the statistics of the lognormally distributed ψ_b and λ (*Rawls et al*. 1982).

Table 1. Summary statistics of G (cm) parameter for various soil types

Soil texture	Arithmetic mean theo.	Arithmetic mean MC	Arithmetic std theo.	Arithmetic std MC	Geometric (MC) mean	Geometric (MC) std
Sand	39	40	118	156	9.9	5.3
Loamy sand	41	44	131	156	12.3	4.8
Sandy loam	64	62	186	153	22.1	4.3
Loam	105	112	475	493	17.9	6.9
Silt loam	158	156	563	544	33.5	5.8
Sandy clay loam	181	180	864	800	44.1	5.
Clay loam	129	129	364	309	42.3	4.5
Silty clay loam	195	183	601	561	55.0	4.9
Sandy clay	219	224	909	937	48.6	5.9
Silty clay	209	204	666	583	59.0	4.9
Clay	242	232	770	689	64.1	5.

Figure 2 plots the theoretical arithmetic mean (analytical) and standard deviation versus those obtained by MC simulations. The comparison shows that the l**ognormal** approximation of G is valid over different soil textures. We note that the results in Table 1 are based on $\psi_i = \infty$, which in light of Equation 8 varies with ψ_i.

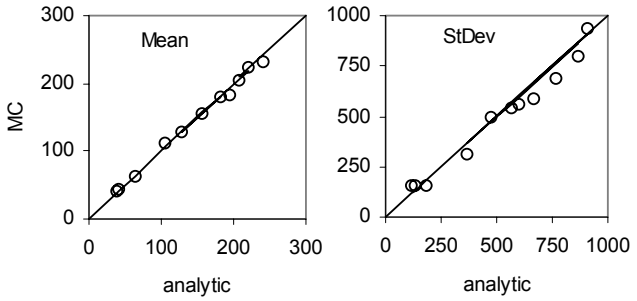

Figure 2. MC versus theoretical mean and std of G.

Monte Carlo Simulations

The objective here is to identify model parameters that have the greatest impact on model output uncertainty, and compare MC results with observations in a small USDA experimental watershed (W-2). The watershed is located near Treynor, Iowa, and has an area of 83 acres (Figure 3).

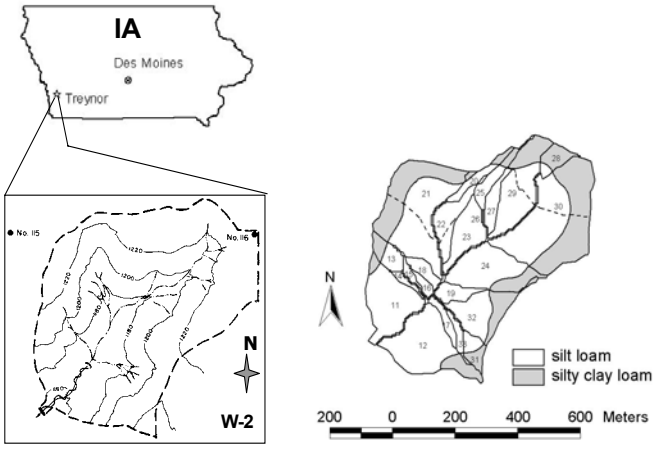

Figure 3. W-2 study watershed (left) and cascade planes, channels, and soil texture class (right).

Two rain gauges (115 and 116) measure rainfall intensity in the watershed. The watershed has a rolling topography defined by gently sloping ridges, steep side slopes, and alluvial valleys with incised channels that normally end at an active gully head (*Kalin et al.* 2003, and references therein). Slopes vary from 2 to 4 percent on the ridges and valleys and 12 to 16 percent on the side slopes. The major soil types are well drained and consist of silt loam (SL) and silty clay loam (SCL) textures that are very prone to erosion, requiring suitable conservation practices to prevent soil loss. Corn has been grown continuously on W-2 since 1964. Figure 3 (to the right) shows spatial extent of soil texture in the W-2 watershed and the overland flow planes, marked by solid line boundaries, used in the simulations. To assess model output response to model input parameters' uncertainty, we performed Monte Carlo simulations using KINEROS2. This is accomplished by generating one thousand set of independently distributed random values of the parameters λ, ψ_b, K_s, S_i, n_c, and n_p, ϕ, c_g, c_f, I, and $D_{50}$from their respective probability distributions, then performing 1000 model runs, one for each randomly generated parameter set. Above, n_c, and n_p, respectively, are the channel and plane Manning's roughness; S_i is the initial soil saturation; ϕ is the soil porosity; I is interception depth; and D_{50} is the median particle size.

Kalin and Hantush (2003), and references therein, provide the range and distributions of key soil and model parameters. We generated the distribution of G parameters using equation (9) and lognormally distributed λ and ψ_b (*Rawls et al.* 1982). Figure 4 shows probability of exceeding peak sediment discharge rate Q_s (Kg/s), sediment yield (tons), and time to peak sediment discharge (min) for each of the above randomly generated parameters λ, G, K_s. S_i, n_c, and n_p. For example, the curves corresponding to K_s are obtained by sampling its values from its lognormal distribution while fixing all other parameters at their mean values. Plane and channel Manning roughness coefficients n_p and n_c are assumed to be uniformly distributed.

A sudden drop from 1 to 0 in the exceedance probability implies no variation of the model output with respect to the particular parameter uncertainty, whereas the more gradual the transition from 1 to 0, the more sensitive the model output to the parameter. Both the peak sediment discharge and sediment yield are highly sensitive to K_s, G, S_i, and n_p, and to a lesser extent to λ (with ψ_b fixed at its geometric mean). Uncertainty in the channel Manning roughness n_c has almost no impact on the model output (a sharp transition from 1 to 0 as shown in Figure 4). Parameter λ mostly affects Q_s and to a lesser extent the sediment yield. We note that sensitivity with respect to λ is more pronounced than what is reported by *Kalin and*

Hantush (2003), which is rather expected, since this parameter generally affects the net capillary drive G parameter. Although λ affects model output only through the G parameter, allowing ψ_b to vary randomly, but independently, with λ explains the more gradual transition from 1 to zero of the probability exceedance curve for G than that for λ, indicating a greater uncertainty of the model output with respect to the former. The Manning roughness coefficients n_p and n_c have the greatest impact on exceedance probability of time to peak sediment discharge, with K_s and G having rather a moderate effect, as the last of Figure 4 shows. S_i and λ have the least effect on the distribution of time to peak sediment discharge rate. Using MC simulations, *Kalin and Hantush* (2003) showed that for large rainfall events, peak sediment discharge and sediment yield is highly influenced by uncertainty in the hydraulic erosion parameter c_g and much less sensitive to the rain splash erosion parameter c_f. What was interesting, however, is that this mode of sensitivity is reversed for smaller events, where rain splash erosion dominates model output uncertainty.

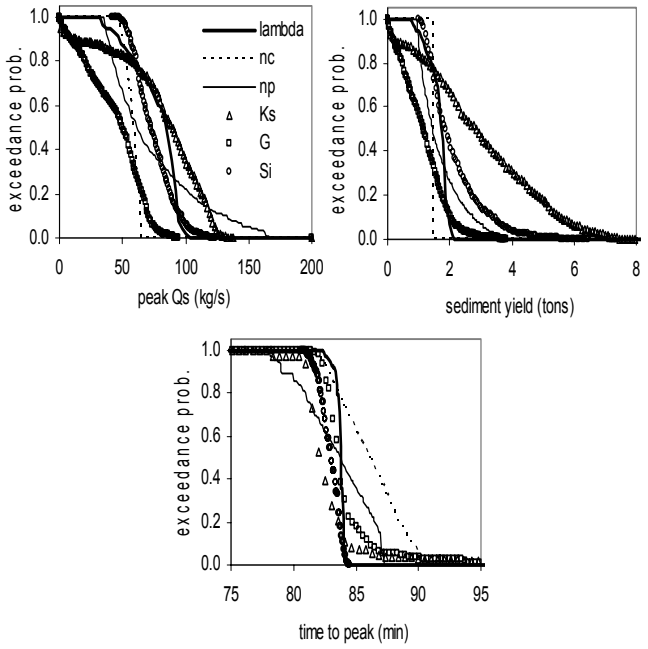

Figure 4. Probability of exceedance of peak sediment discharge rate (Kg/s), sediment yield (tons), and time to peak sediment discharge (min) for different randomly distributed parameters.

Figure 5 shows the median, 25% quartile values, 5% quartile values, and observations of runoff Q_f and sediment discharge Q_s for the large and small rainfall events shown in Figure 6. The 75% and 95% quartile values, which along with the 25% and 5% quartile values bracket the 50% and 90% confidence intervals, respectively, are not shown for the purpose of clarity. The results are obtained by performing MC simulations with all of the above model parameters, including $c_g \sim$ Uniform(0.01-1 s^{-1}) and $c_f \sim$Uniform(100-1000 s), randomly varied. The two extreme values of Parlange et al. infiltration parameter α are used; i.e., α = 0 and 1. Although α = 0.85 is recommended (*Parlange et al.*, 1982), the results in Figure 5 shows that this parameter has almost no impact on the median of both runoff and sediment discharge except in the vicinity of peak values. For both events, the median significantly over estimated the observed Q_f and Q_s during the rising parts of the hydrograph and sedimentograph and early portions of the recession curve. It is remarkable that the median, and without calibration, simulated fairly well the observed values of the flow and sediment discharge rates during later portions of the recession; roughly, during the time period from 90th to the 120th minutes for the larger of the two events in Figure 7, and from 70th to 100th minute for the smaller event. Overall, the median of both runoff and sediment discharge rates are within order of magnitudes of the observed values for the larger event. More than 50% of the observations are within the median (± 25% quartile values). Within this confidence interval, the probability is 50% that flow or sediment discharge would be observed, provided that the model approximates the underlying physical processes reasonably well. All measurements fall within the 90% confidence interval, corresponding to the median ±45% quartile values.

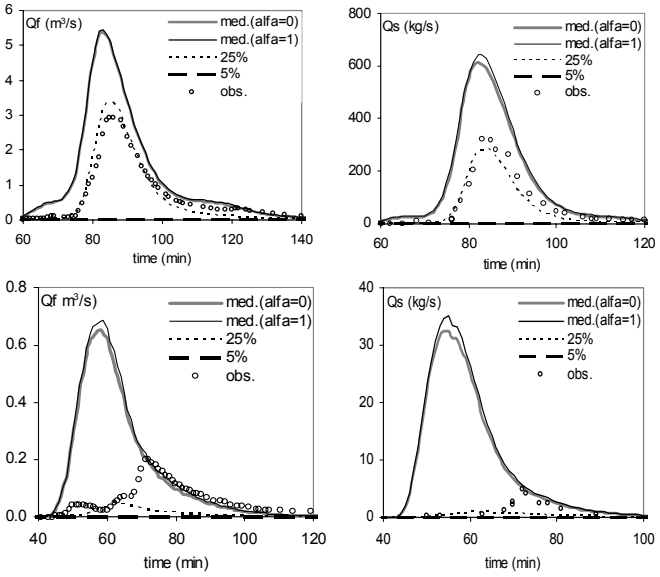

Figure 5. MC simulations for large (top two) and small (bottom two) rainfall events: median and quartiles

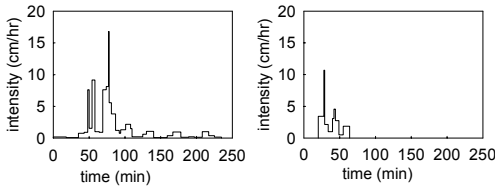

Figure 6. Rainfall events at 6/13/83 (left) and 8/26/81 (right).

Conclusions

This paper applied the event-, physically-based, and distributed runoff/erosion model KINEROS2 to an experimental watershed in Iowa. The net capillary drive, G, parameter is a key parameter to this model, which affects both runoff and sediment transport. Statistics of the net capillary drive parameter were obtained and tabulated for all soil texture classes. These values can be used in future applications of KINEROS2. Monte Carlo simulations were conducted to assess the impact of uncertainty in model parameters on the variation of sediment discharge rate, sediment yield, and time to peak sediment discharge rate. Comparison with observations of runoff and sediment discharge rates of the median, median ± 25% and ±45% quartile values, obtained by performing Monte Carlo simulations indicated that KINEROS2 performed well given the uncertainties in model parameters as reported in the literature. The model can be calibrated successfully without fear of producing artifact model parameters.

Acknowledgements

The U.S. Environmental Protection Agency through its Office of Research and Development funded and managed the research described here through in-house efforts. This research was supported in part by an appointment to the Postgraduate Research Program at the National Risk Management Research Laboratory administered by the Oak Ridge Institute for Science and Education through an interagency agreement between the U.S. Department of Energy and the U.S. Environmental Protection Agency. The authors thank Dennis Lai and Mingyu Wang for reviewing the manuscript.

Reference

Engelund, F., and E. Hansen. 1967. A monograph on sediment transport in alluvial streams. Teknisk Vorlag, Copenhagen.

Kalin, L., and M. M. Hantush. 2003. Modeling of sediment yield in a small agricultural watershed with KINEROS2. *In* J. D. Williams and D. W. Koplin, ed., American Water Resources Association 2003 Spring Specialty Conference on Agricultural Hydrology & Water Quality, Kansas City, MO, CD-ROM.

Kalin, L., R.S. Govindaraju, M.M. Hantush. 2003. Effect of geomorphologic resolution on runoff hydrograph and sedimentograph. J. Hydrol. 276: 89-111.

Osborn, H.B., and J.R. Simanton. 1990. Hydrologic modeling of a treated rangeland watershed. Journal of Range Management 43:474-481.

Parlange, J.-Y., I. Lisle, and R.D. Braddock. 1982. The three-parameter infiltration equation. Soil Science 133:337-341.

Rawls. W.J., D.L. Brakensiek, and K.E. Saxton. 1982. Estimation of Soil Water Properties. Transactions of the ASAE 81-2510:1316-1328.

Smith, R.E., D.C. Goodrich, D.A. Woolhiser and C.L. Unkrich. 1995. A kinematic runoff and erosion model. *In* V.J. Singh, ed., Computer Models of Watershed Hydrology, 697-732, Water Resources Pub., Highlands Ranch, CO.

Smith, R.E., D.C. Goodrich and C.L. Unkrich. 1999. Simulation of selected events on the Catsop catchment by KINEROS2. A Report for the GCTE Conference on Catchment Scale Erosion Models. Catena 37: 457-475.

U.S.EPA 2000. The Quality of Our Nation's Waters. A Summary of the National Water Quality Inventory: 1998 Report to Congress. Office of Water, Washington, DC. 841-S-00-001.

Woolhiser, D.A., R.E. Smith and D.C. Goodrich. 1990. KINEROS-A kinematic runoff and erosion model: Documentation and user manual. USDA-ARS, ARS-77, pp. 130.

Ziegler, A.D., T.W. Giambelluca, and R. A. Sutherland. 2001. Erosion prediction on unpaved mountain roads in northern Thailand: Validation of dynamic erodibility modeling using KINEROS2. Hydrological Processes 15:337-358.